TELKOMNIKA Telecommunication Computing Electronics and Control
Vol. 24, No. 1, February 2026, pp. 258~270
ISSN: 1693-6930, DOI: 10.12928/TELKOMNIKA.v24i1.27330

Optimized IMC with GWO algorithm and variable switching function for voltage regulation of SEPIC converter

Reza Fazeli[1], Mohammad Haddad Zarif[1], Mahmoud Zadehbagheri[2], Tole Sutikno[3,4]
[1]Department of Electrical and Robotic Engineering, Shahrood University of Technology, Shahrood, Iran
[2]Department of Electrical Engineering, Yasuj branch, Islamic Azad University, Yasuj, Iran
[3]Master Program of Electrical Engineering, Faculty of Industrial Technology, Universitas Ahmad Dahlan, Yogyakarta, Indonesia
[4]Embedded System and Power Electronics Research Group, Yogyakarta, Indonesia

Article Info

Article history:

Received Jun 29, 2025
Revised Nov 13, 2025
Accepted Dec 8, 2025

Keywords:

Delayed systems
Internal model control
Optimization
Single-ended primary-inductor converter
Variable switching function

ABSTRACT

With the growing application of single-ended primary-inductor converter (SEPIC) converters in power electronic systems, precise output voltage regulation under uncertainties and nonlinear conditions remains a significant challenge. Although internal model control (IMC) effectively addresses issues arising from unstable zeros and fixed time delays in non-minimum phase systems, its performance can degrade under large transient errors or sudden disturbances, leading to control signal saturation and instability. In this study, a modified IMC scheme is proposed, which integrates a variable switching function into the control structure. This addition enhances the robustness of the system by dynamically adapting the control effort to mitigate abrupt changes in the control signal and stabilize the output voltage. Furthermore, it prevents controller saturation during large-signal deviations, thereby improving transient response and maintaining system stability. The design parameters of the controller are optimized using the gray wolf algorithm to achieve an optimal balance between voltage overshoot, settling time, and closed-loop stability. Simulation results under various operating conditions confirm the superior performance of the proposed control method compared to conventional IMC.

Corresponding Author:

Reza Fazeli
Department of Electrical and Robotic Engineering, Shahrood University of Technology
Shahrood, Iran
Email: r.fazeli1000@gmail.com

1. INTRODUCTION

Modern energy and transportation systems depend on power electronic converters to efficiently convert and manage electrical power for many uses. They efficiently scale voltage levels up or down, enabling power supply and load integration. The single-ended primary inductor converter (SEPIC) is a crucial converter topology for applications needing a variable output range. Adjusting the duty cycle allows the SEPIC converter to generate an output voltage lower, equal to, or greater than its input while retaining non-inverted polarity. It can buck and boost with minimal input current ripple and a ground-referenced switch [1].

Power converters, especially SEPIC converters, need precise management to maximize performance. Direct current to direct current (DC–DC) converters are nonlinear, time-varying systems, and the SEPIC architecture makes control plant design difficult. A fourth-order system with complicated dynamics makes controller design and stability analysis difficult. Like other boost-derived converters, the continuous-conduction-mode SEPIC has a right-half-plane zero in its control-to-output transfer function [2]. The right-half-plane (RHP) zero creates an initial inverse reaction (output drops while duty rises) and a 180°

phase lag, severely restricting control bandwidth. RHP zero and higher-order resonances of the SEPIC might impede closed-loop responses or cause instability if not adequately accounted for [3]. In practice, the converter must maintain a constant regulated output despite input voltage changes and load transients. A robust controller must reject disruptions from solar panels or batteries and maintain output in renewable energy applications. Normal linear controllers built for small-signal models typically fail under large-signal fluctuations. The SEPIC converter needs sophisticated control algorithms to achieve quick transient response, little overshoot, and high disturbance rejection [4]. In conclusion, the SEPIC's nonlinear and non-minimum-phase features make high-precision control vital and difficult, prompting substantial study into converter control methods [5]–[7].

Nonlinear, variable-structure resilience DC–DC converters employ sliding mode control (SMC). SMC uses a switching control rule to keep the system's state trajectory on a "sliding surface" insensitive to shocks and parameter changes. Because SMC handles nonlinear behavior and huge signal shifts, SEPIC converters perform better than linear controllers. A real SEPIC converter's control input (duty cycle) is limited to 0 and 1 and varies only at the switching frequency, which must be addressed in design. SMC with fixed-frequency modulation or smoothing filters may operate for SMC. High-reliability applications employ SEPIC converters because they can withstand huge shocks and component uncertainties. SMC provides stronger regulation and stability margins than linear controllers but requires a more sophisticated switching-type control rule to prevent chattering [7].

Online controller settings are updated via adaptive control to response to system or environmental changes. SEPIC converter performance can be maintained in all conditions with adaptive control due to its sensitivity to parameter and operating-point adjustments. Adaptive sliding control (ASC) SEPIC provides adaptive SMC. Self-tuning controllers dynamically change sliding surfaces or control gains to reduce noise and increase robustness. As said, SMC chattering needs aggressiveness switching. Adaptive sliding mode control (ASMC) approaches meet sliding mode criteria without extra control effort by restricting switching magnitude to the lowest permissible level [8]. The controller may smooth converter control in calm conditions and push to high gain (and chattering) during major interruptions in real time. This adaptability maintains sliding mode's endurance and performance in different circumstances with minimum chattering. Adaptive SMC designs for SEPIC converters moderate input voltage variations quicker and with less overshoot than fixed SMC laws by changing the sliding surface slope [9]. Gain scheduling modifies proportional–integral–derivative (PID) gains by operating area, and model reference adaptive control (MRAC) requires the converter to follow an adaptive reference model behavior. The researcher used MRAC on SEPIC converters to control unexpected load levels and maintain a reference dynamic output voltage. Self-tuning regulators alter controller settings via neural networks or fuzzy logic. SEPIC adaptive control manages system uncertainty and drift reliably [10]. In adaptive SMC, variable-structure robustness and adaptive tracking provide online learning and control. Adaptive schemes may challenge the controller design and the adaptation mechanism. Overshooting and adaptive law convergence need research or design. Thus, the adaptive controller must operate quickly. Modern digital processors can accomplish this, making the design harder. SEPIC converters benefit from adaptive control in wide-range or unpredictable settings. Online controllers may self-tune to enhance SEPIC performance across their operational envelope, unlike fixed-gain controllers [11].

High-resolution digital pulse-width modulators (DPWMs) and analog-to-digital converters (ADCs) enhance digital control of SEPIC converters by addressing sampling and synchronization challenges. Co-designing the converter and controller simplifies the system, with current-mode control and coupled inductors reducing unwanted high-order effects. Effective digital algorithms require a stable analog power stage, enabling SEPIC converters to implement advanced inner current and outer voltage loops. Digital control allows for high-performance, adaptive, and reliable SEPIC regulation when designed with proper synchronization and consideration of sampling effects [12]–[14]. Shawky *et al*. [15], a non-isolated dual-input converter is proposed for simultaneous use of solar cells alongside energy storage systems. The proposed structure is a combination of a buck-boost converter and a boost converter, which consists of four power switches and four diodes. Zadehbagheri *et al*. [16], a new non-isolated dual-input converter is also proposed, which, due to the direct connection of the inputs and the output to each other, is only used in contexts where isolation of the output from the inputs is not required. Al Sakka *et al*. [17], considers a digital control method for the optimal time-dependent loading stage response of SEPIC converters for point-of-loading applications using low ESR output capacitors. Tuan *et al*. [18], a converter with a combined structure of capacitive switching and inductive switching along with a classic SEPIC converter is presented. This converter has a high voltage gain but the current stress and voltage stress on the power switches are high. Gao *et al*. [19], a new DC-DC converter with SEPIC structure without using coupling inductor with high voltage gain is proposed, which has high efficiency and high converter reliability. The proposed converter is suitable for use in photovoltaic (PV). Zadehbagheri *et al*. [20], a PV system controlled using two tracking algorithms perturb and observe (P&O) (traditional method) and Fuzzy logic–based proportional–integral

controller (Fuzzy-PI) (intelligent method) for maximum power point tracking (MPPT) controller is presented. In addition, in the control signal application section, a SEPIC converter is used. This system is studied under normal weather conditions and partial shade.

In this study, a novel control approach is proposed for the SEPIC converter: an internal model control (IMC) strategy optimized by the gray wolf (GWO) algorithm, integrated with a variable switching function. This innovative scheme combines the strength of IMC, known for excellent disturbance rejection and handling of non-minimum-phase systems, with a variable switching function concept that enhances control flexibility and robustness. The GWO optimization metaheuristic is employed to automatically tune the IMC parameters and the switching function, ensuring optimal closed-loop pole placement and dynamic response. By merging a variable-structure control element with an optimally tuned IMC, the proposed controller achieves superior voltage regulation performance for the SEPIC converter, offering improved stability and transient response beyond what conventional PID, SMC, or other existing methods can deliver [15], [20].

2. METHOD

2.1. Modeling of a SEPIC converter

Selecting an appropriate DC-DC converter topology depends on factors such as switching losses, voltage gain, output current and power levels, cost, operating modes, and application requirements. The SEPIC offers distinct advantages over other types, including reduced input current ripple and electrical isolation between input and output via a series capacitor. Its non-inverting output and versatility enable both step-up and step-down operation, as shown in Figure 1.

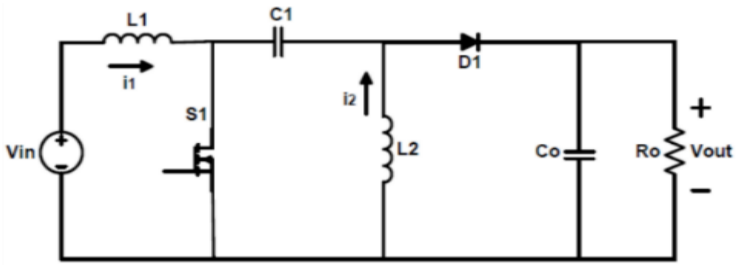

Figure 1. Structure of SEPIC

A notable characteristic of the SEPIC converter is its phase-independent behavior, exhibiting a known output delay that introduces a RHP zero in the transfer function. This RHP zero complicates control by limiting gain, slowing response, and increasing the risk of overshoot, oscillation, or instability. These challenges underscore the need for advanced control strategies tailored to the SEPIC converter's unique dynamics [15], [16], [21].

A conventional SEPIC converter can be divided into three segments in view of the power conversion and control process of the converter. At the first segment, ac to dc rectification is accomplished using a traditional diode bridge. However, instead of a diode bridge, alternating current (AC) to DC rectification can also be achieved with semiconductor switches in bird geless SEPIC configuration. In the second stage, high–frequency switching operation is performed. As a result of this stage, the output power either decreases (buck operation) from the input or increases (boost operation) depending on the duty ratio of the switch. The final stage before the output is the remaining portion of the DC–DC SEPIC converter, consisting of reactive elements and an associated freewheeling diode. The configuration of the SEPIC converter varies based on the state of the control signal, which alternates between zero and one. This switching action alters the conduction paths within the circuit, resulting in different operating modes as illustrated in Figure 2 [22], [23].

In Figure 2(a), the SEPIC converter operates with a control signal of one, activating the switch and turning the diode off. In contrast, Figure 2(b) depicts the switch in the off state (control signal zero), allowing the diode to conduct. For modeling simplicity, both the switch and diode are idealized as short circuits when conducting and open circuits otherwise thus ignoring switching and conduction losses. By applying Kirchhoff's laws to these two states, switching equations are derived to describe the converter's dynamic behavior under both conditions of the control signal D [20], [22].

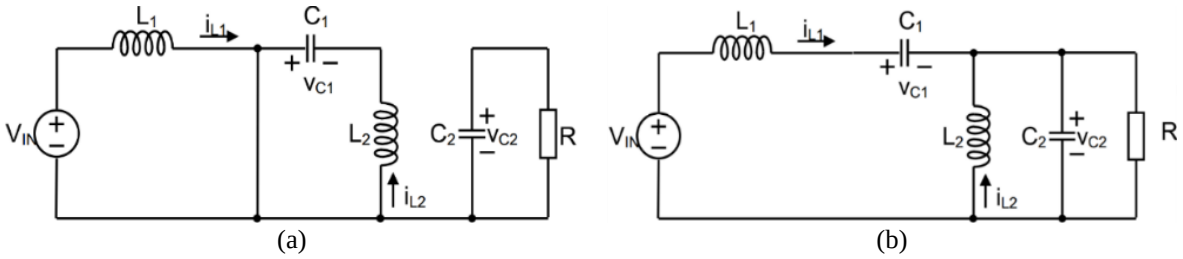

Figure 2. Equivalent circuit of the SEPIC converter in the case of (a) control signal one and diode off and (b) control signal zero and diode on

$$\begin{cases} I_{\dot{L}1} = -\frac{(1-D)}{L_1}(V_1 + V_2) + \frac{V_{in}}{L_1} \\ V_{\dot{1}} = \frac{(1-D)}{C_1} I_{L1} - \frac{D}{C_1} I_{L2} \\ I_{\dot{L}2} = \frac{u}{L_2}(V_1 + V_2) - \frac{V_2}{L_2} \\ V_{\dot{2}} = \frac{(1-D)}{C_2}(I_{L1} + I_{L2}) - \frac{V_2}{RC_2} \end{cases} \quad (1)$$

Followed by small-signal modeling around these points. This approach addresses nonlinearities from the input voltage and control signal interactions by assuming small perturbations. As a result, a linearized state-space model with the control signal as input is derived.

$$\begin{bmatrix} \frac{d\tilde{\imath}_{L1}}{dt} \\ \frac{d\tilde{\imath}_{L2}}{dt} \\ \frac{d\tilde{v}_{C1}}{dt} \\ \frac{d\tilde{v}_{C2}}{dt} \end{bmatrix} = \begin{bmatrix} 0 & 0 & -\frac{1-D}{L_1} & -\frac{1-D}{L_1} \\ 0 & 0 & -\frac{D}{L_2} & \frac{1-D}{L_2} \\ \frac{1-D}{C_1} & \frac{D}{C_1} & 0 & 0 \\ \frac{1-D}{C_2} & -\frac{1-D}{C_2} & 0 & -\frac{1}{RC_2} \end{bmatrix} \begin{bmatrix} \tilde{\imath}_{L1} \\ \tilde{\imath}_{L2} \\ \tilde{v}_{C1} \\ \tilde{v}_{C2} \end{bmatrix} + \begin{bmatrix} \frac{v_{in}+v_{out}}{L_1} \\ -\frac{v_{in}+v_{out}}{L_2} \\ \frac{i_{L2}-i_{L1}}{C_1} \\ \frac{i_{L2}-i_{L1}}{C_2} \end{bmatrix} \tilde{d} \quad (2)$$

$$y = [0 \quad 0 \quad 0 \quad 1] \begin{bmatrix} \tilde{\imath}_{L1} \\ \tilde{\imath}_{L2} \\ \tilde{v}_{C1} \\ \tilde{v}_{C2} \end{bmatrix}$$

As observed, capacitor C2 is connected in parallel with the output load, which means the voltage across C2 directly represents the converter's output voltage. Consequently, in the state-space representation, the output matrix C is defined as [0 0 0 1], indicating that only the state corresponding to the voltage across C2 contributes to the output. Based on this configuration, the transfer function that relates the control input (the duty cycle D) to the output voltage can be derived accordingly.

$$H_{\tilde{d}\to v_{C2}}(s) = \frac{b_3 s^3 + b_2 s^2 + b_1 s + b_0}{s^4 + a_3 s^3 + a_2 s^2 + a_1 s + a_0} \quad (3)$$

The numerator and denominator parameters of the SEPIC converter's transfer function are derived from its physical components, including inductance, capacitance, load resistance, and switching frequency. These parameters define the system's dynamic characteristics by determining the locations of poles and zeros. Notably, the presence of a RHP zero arising from the converter's inherent structure affects the phase response and complicates controllability, making accurate modeling essential for effective control design [24], [25].

$$\begin{aligned} b_0 &= (1-\alpha_e)\frac{v_{C1e}+v_{C2e}}{L_1 L_2 C_1 C_2} \\ b_1 &= -\alpha_e L_1 \frac{i_{L1e}+i_{L2e}}{L_1 L_2 C_1 C_2} \\ b_2 &= (1-\alpha_e)\frac{v_{C1e}+v_{C2e}}{L_1 L_2 C_1 C_2}(L_1 + L_2)C_1 \\ b_3 &= -\frac{i_{L1e}+i_{L2e}}{C_2} \end{aligned} \quad (4)$$

$$a_0 = \frac{(1-\alpha_e)^2}{L_1L_2C_1C_2}$$
$$a_1 = \frac{1}{R} \cdot \frac{\alpha_e^2L_1+(1-\alpha_e)^2L_2}{L_1L_2C_1C_2} \quad (5)$$
$$a_2 = \frac{(1-\alpha_e)^2(L_1C_1+L_2C_2+L_2C_1)+\alpha_e^2L_1C_2}{L_1L_2C_1C_2}$$
$$a_3 = \frac{1}{RC_2}$$

An examination of the fractional form presented in (3) reveals the existence of an unstable zero, specifically, an RHP zero in the transfer function. This RHP zero introduces a phase lag and is functionally equivalent to a constant time delay in the system's output response. As a result, the SEPIC converter exhibits non-minimum phase behavior, meaning that its output voltage initially responds in the opposite direction of the intended change when the control signal is varied. This dynamic characteristic poses a challenge for controller design, particularly in achieving fast and stable regulation. Utilizing the parameter values specified in Table 1, the open-loop transfer function of the system is derived and presented as (6).

Table 1. Parameters values of the SEPIC converter

Parameter	Values
V_{in}	12 V
V_{out}	24 V
C_1	30 µF
C_2	192 µF
L_1	20 µH
L_2	100 µH
R_o	10 ohms
Switching frequency	30 kHz

$$G(s) = \frac{-(3.75*10^4)s^3+(3.75*10^9)s^2-(8.33*10^{12})s+(1.04*10^{18})}{s^4+(520.8)s^3+(3.68*10^8)s^2+(1.73*10^{11})s+(9.64*10^{15})} \quad (6)$$

2.2. Design of the internal model controller

The IMC approach is especially effective for systems with phase-independent behavior and known time delays, such as the SEPIC converter. These systems often feature a RHP zero, representing an intrinsic delay that complicates traditional control design. IMC overcomes this challenge by explicitly modeling the system delay and integrating it within the control architecture, thereby enabling improved stability and performance in the presence of non-minimum phase dynamics. To address the challenges posed by the SEPIC converter's unstable zero, the system's transfer function is decomposed, enabling the design of a tailored controller that accounts for its non-minimum phase characteristics. A key element in this design is a tuning parameter that dictates closed-loop pole placement and influences overall dynamic response. This parameter is optimized using the GWO algorithm to strike a balance among key transient performance indicators, including overshoot, settling time, and stability. Figure 3 presents the block diagram of the proposed control scheme, illustrating the IMC framework and its components. The diagram depicts the signal flow, the integration of the system model and filter design, the treatment of disturbances, and the optimization process, offering a comprehensive view of the control architecture.

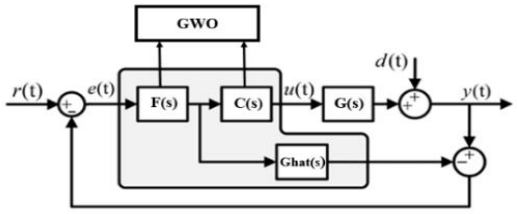

Figure 3. Block diagram of the proposed method

In the proposed control structure illustrated in Figure 3, the various components serve the following roles: $r(t)$ denotes the reference signal, $e(t)$ is the error computed as the difference between the output $y(t)$

and the reference input $r(t)$, $d(t)$ represents external disturbances acting on the system, $y(t)$ is the actual system output, GWO refers to the GWO algorithm used for tuning the controller parameters, $C(s)$ is the internal model controller to be designed, $F(s)$ is a low-pass filter constructed based on the nature of the reference signal to ensure realizability and robustness, $G(s)$ represents the actual transfer function of the SEPIC converter, and $G_{hat}(s)$ denotes the model used within the controller structure (i.e., the internal model).

To construct the internal model controller, the open-loop transfer function obtained in (6) must be decomposed into two separate transfer functions: $G+(s)$, which encapsulates the non-minimum phase components, including the unstable zero and time delay, $G-(s)$, which includes the remaining stable dynamics of the system. Based on the above, the (7) is written.

$$\begin{aligned} G(s) &= G_{-}G_{+} \\ G_{-} &= \frac{-(37500)s^3-(3.79*10^9)s^2-(1.24*10^{13})s-(1.04*10^{18})}{s^4+(520.8)s^3+(3.68*10^8)s^2+(1.73*10^{11})s+(9.64*10^{15})} \\ G_{+} &= \frac{s-100540}{s+100540} \end{aligned} \tag{7}$$

As shown in Figure 3, the internal model controller $C(s)$ is derived by inverting the stable part of the system transfer function $G(s)$, as defined in (8). This inversion enables accurate compensation of predictable plant dynamics. A filter $F(s)$, defined in (9), is then applied to shape the controller's frequency response. The filter order nnn and tuning parameter λ influence the closed-loop pole locations and bandwidth, ensuring controller realizability and preventing non-causal or overly aggressive behavior. The final IMC-based controller $Q(s)$ is constructed by combining $C(s)$ and $F(s)$, as shown in (10). This final controller $Q(s)$ governs the system's control law, and its performance is heavily dependent on the choice of the design parameter λ. The parameter is subsequently optimized using the GWO algorithm to achieve the desired transient and steady-state characteristics.

$$C(s) = G(s)_{-}^{-1} \tag{8}$$

$$F(s) = \frac{G(0)_{+}^{-1}}{(1+\lambda s)^n} \tag{9}$$

$$Q(s) = F(s)C(s) \tag{10}$$

By optimizing the controller $Q(s)$ with respect to the tuning parameter λ, the location of the closed-loop poles can be strategically adjusted to ensure a stable and responsive output voltage in the SEPIC converter. The parameter λ directly influences the dynamics of the filter $F(s)$, and thus plays a critical role in determining the system's transient behavior, including settling time, overshoot, and robustness to disturbances. To achieve optimal performance, the GWO algorithm is employed to determine the most suitable value of λ automatically.

2.3. Gray wolf algorithm

The GWO algorithm is a bio-inspired metaheuristic that simulates the social hierarchy and cooperative hunting strategies of gray wolves. It categorizes wolves as alpha, beta, delta, and omega, with the top-ranking wolves guiding the search toward the global optimum symbolized as prey. Wolves iteratively adjust their positions based on the leaders' guidance, balancing exploration and exploitation throughout the search space. This strategy enables GWO to efficiently handle complex, nonlinear, and high-dimensional optimization problems, making it particularly effective for tuning control parameters in dynamic systems like power converters [17]–[19]: i) strong global search capability with balanced exploration and exploitation; ii) simple implementation with few control parameters; iii) high convergence speed in nonlinear problem domains; iv) robustness in avoiding local optima; and v) adaptability to diverse engineering applications, including real-time control systems. These characteristics make the GWO algorithm particularly well-suited for optimizing IMC parameters in SEPIC converters, where achieving a balance between stability, dynamic responsiveness, and robustness is essential. GWO has gained increasing prominence for its effectiveness in addressing complex, nonlinear optimization tasks with high reliability and computational efficiency. In this study, GWO is applied during an offline optimization phase, subsequent to the initial IMC design. The primary objective is to determine the optimal tuning parameter λ, which directly influences the placement of the closed-loop poles and thus governs the system's dynamic behavior affecting stability, transient speed, and robustness. Figure 4 shows the flowchart of the GWO algorithm with details on the optimization process.

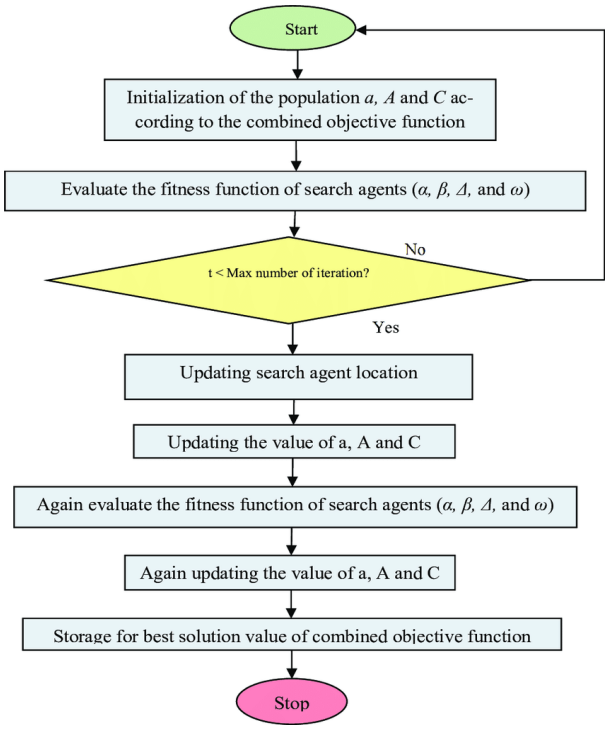

Figure 4. Flowchart of the GWO algorithm

To evaluate performance and guide the optimization, a cost function T, defined in (11) is formulated. This function integrates three essential performance indices to quantify and enhance the SEPIC converter's output voltage regulation: voltage overshoot, settling time, closed-loop stability index.

$$T = W_1(\mathrm{OS}) + W_2(\mathrm{ST}) + W_3(\mathrm{SI}) \quad (11)$$

Where, T: total cost function value to be minimized, OS: overshoot in the output voltage, ST: settling time of the output response, SI: stability index, reflecting how well the system maintains stability under perturbations, W_1, W_2, W_3: weighting coefficients that determine the relative importance of each performance metric. By appropriately selecting the weights W1, W2, and W3, the cost function can be tailored to prioritize specific aspects of performance (speed vs robustness), enabling the GWO algorithm to find the optimal value of λ that delivers the best overall control behavior for the SEPIC converter.

Each component is weighted according to its relative importance, enabling the optimization to target a balanced trade-off between speed and stability. The parameter λ is constrained within the range $0.001 < \lambda < 1$ to ensure practical realizability and system responsiveness. Table 2 outlines the definitions and values of the optimization parameters, including the number of iterations, population size (number of wolves), and weights assigned to each term in the cost function. Figure 5 illustrates the convergence behavior of the optimization process, demonstrating the progressive reduction of the cost function over iterations. This confirms the effectiveness of the GWO algorithm in identifying a near-optimal controller configuration for the SEPIC converter [19], [25], [26].

Table 2. Optimization parameters

Parameter	Values
Number of steps	100
Number of wolves	50
OS	Overshoot
ST	Settling time
SI	Stability index
W_1	voltage overshoot weight
W_2	Settling time weight
W_3	Stability index weight
λ	0.005

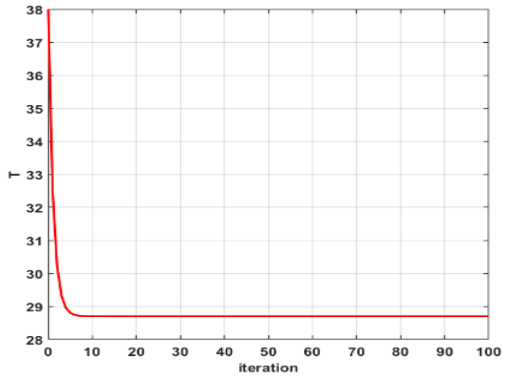

Figure 5. Cost function reduction graph versus stage

2.4. Integration of variable switching frequency with optimized internal model control

While the GWO algorithm–optimized internal model controller offers a solid foundation for handling the SEPIC converter's non-minimum phase characteristics, integrating a variable switching frequency mechanism further enhances system performance. This strategy modulates switching frequency in proportion to the control error magnitude, enabling rapid response to large deviations and minimizing switching in steady states. By linking frequency adjustment to the absolute output-reference voltage error, the method effectively tackles two key challenges in power converter control: improving transient responsiveness and reducing switching losses:

- Improved dynamic response during large transients by increasing the switching frequency, thereby enhancing control granularity and responsiveness.
- Reduced switching losses and stress under near-steady-state operation by lowering the frequency, contributing to greater efficiency and reliability.

The proposed switching frequency f_s is defined as:

$$f_s(t) = f_{\text{base}} \cdot W \cdot |e(t)| \tag{12}$$

where: $f_s(t)$: instantaneous switching frequency at time t, f_{base}: base switching frequency under nominal conditions, W: design weight determining the sensitivity of frequency modulation, $|\ e(t)\ |$: absolute value of the control error at time t.

The proposed formulation dynamically adjusts the switching frequency based on the tracking error magnitude. During significant disturbances such as abrupt load or input changes the frequency increases, enabling finer control and faster error correction. In steady-state conditions, the frequency decreases to reduce switching losses. Key advantages of this hybrid control approach include:

- Improved voltage stability with smooth transitions and minimal overshoot
- Lower control signal oscillations and reduced risk of actuator saturation
- Automatic adaptability to changing operating conditions without manual tuning
- Enhanced energy efficiency by limiting switching during low-error states

The variable switching mechanism operates alongside the IMC–GWO control loop, using the error signal to modulate switching frequency in real time. This integration unites model-based precision with adaptive responsiveness, achieving robust voltage regulation under diverse conditions.

3. RESULTS AND DISCUSSION

Figure 6(a) shows the SEPIC converter's output voltage under a non-optimized internal model controller with fixed switching frequency. While aiming for a constant 10 V reference, the controller exhibits slow rise time and fails to reach the target within 1 second, resulting in steady-state error. The output displays step-like increments and prominent high-frequency oscillations, indicating poor damping and limited dynamic performance. These deficiencies underscore the necessity of controller optimization and adaptive switching frequency to improve voltage regulation accuracy, stability, and responsiveness. Figure 6(b) illustrates the SEPIC converter's output voltage response in step-down mode, where a lower reference is tracked. The proposed controller an Internal model controller optimized by the GWO algorithm with variable switching frequency achieves fast settling, minimal overshoot, and low steady-state error. Adaptive switching

frequency enhances transient performance by increasing control resolution during high-error periods. Voltage regulation remains stable with bounded oscillations, and control input avoids saturation despite abrupt transitions. These results confirm the method's robustness and precision in managing the SEPIC converter's right-half-plane zero during step-down operation.

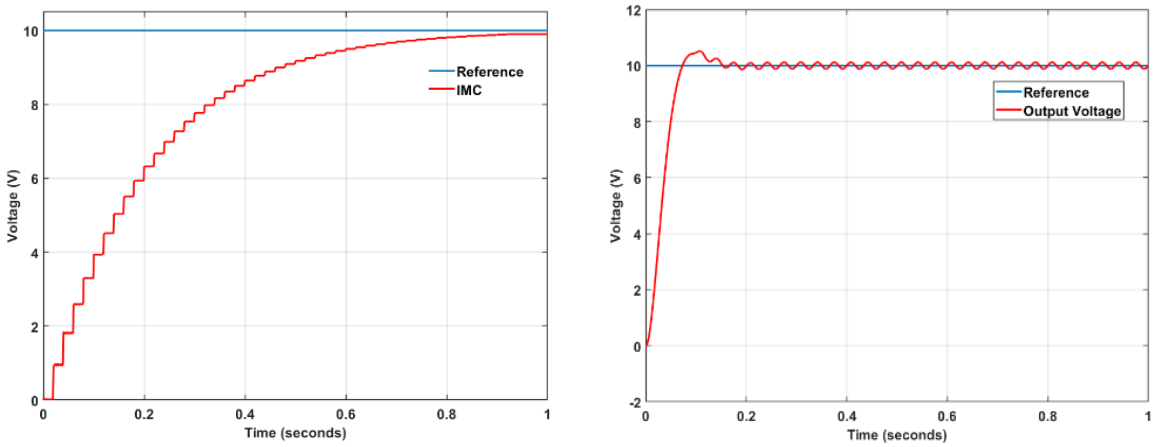

(a) (b)

Figure 6. SEPIC converter's output voltage: (a) output voltage response using non-optimized IMC with fixed switching frequency and (b) output voltage tracking based on reference in step-down mode

Figure 7(a) shows the SEPIC converter operating in boost mode, raising the output above the input voltage. The proposed controller an Internal model controller optimized by the GWO algorithm with variable switching frequency achieves fast and accurate tracking of the 24 V reference. The output stabilizes within 0.15 s with minimal overshoot and negligible steady-state error. Adaptive switching frequency enhances transient response and control resolution, while bounded high-frequency oscillations indicate a well-managed trade-off between switching efficiency and stability. Figure 7(b) illustrates the output voltage behavior of the SEPIC converter under external disturbances, including white noise and a step change in reference. Despite these conditions, the proposed controller combining an Internal model controller optimized via the GWO algorithm and variable switching frequency demonstrates strong robustness. It achieves rapid convergence to both 10 V and 24 V reference levels with minimal overshoot and sustained tracking accuracy, indicating effective disturbance rejection and dynamic adaptability.

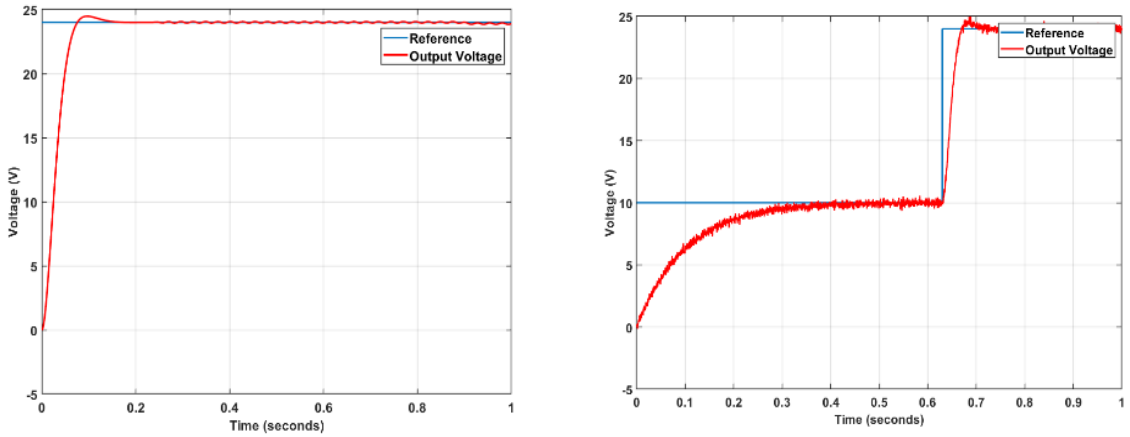

(a) (b)

Figure 7. Output voltage: (a) output voltage tracking based on reference in boost mode and (b) output voltage tracking based on a reference in noise mode with variance 0.1 and step reference

Figure 8(a) presents the SEPIC converter's response to a sudden load decrease from 10 Ω to 5 Ω, simulating high-demand conditions. The proposed control strategy based on an Internal model controller optimized by the GWO algorithm and enhanced by variable switching frequency ensures robust voltage regulation. The output initially tracks the 10 V reference with minimal overshoot. Following the load step, a brief voltage sag occurs but is rapidly corrected with negligible undershoot. Increased switching frequency during error peaks enhances transient response. The system re-stabilizes with minimal ripple, confirming the controller's effectiveness under dynamic, nonlinear loading. Figure 8(b) depicts the SEPIC converter's output response as the input voltage increases from 17 V to 20 V over 0.5 seconds, assessing performance under input-side disturbances. The proposed controller featuring a GWO algorithm-optimized Internal model controller and variable switching frequency achieves rapid tracking of the 24 V reference with minor overshoot and ripple. During the input step, a brief deviation occurs, followed by smooth recovery. Adaptive switching frequency enhances transient correction. The system stabilizes promptly without steady-state error or oscillation, demonstrating strong input disturbance rejection and reliable voltage regulation in fluctuating supply conditions.

Table 3 compares the proposed method with existing SEPIC converter control strategies. conventional PID controllers are simple to implement but perform poorly under nonlinear dynamics and right-half-plane zero, yielding limited steady-state precision and weak disturbance rejection. SMC enhances robustness and handles nonlinearity but suffers from chattering and implementation complexity.

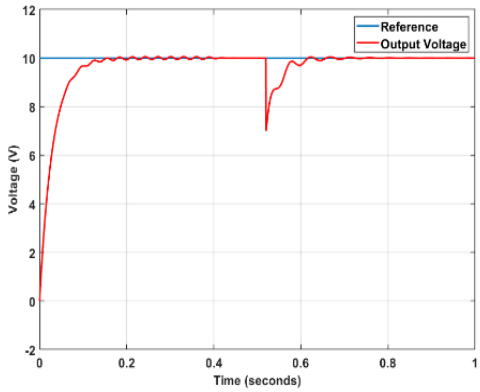

(a)

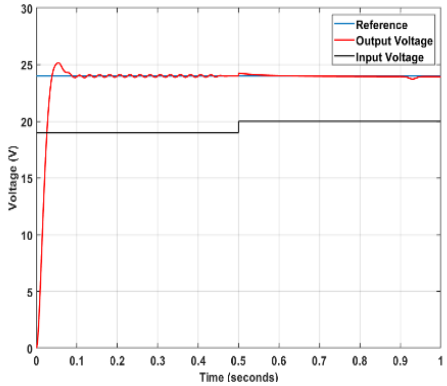

(b)

Figure 8. Output voltage tracking: (a) output voltage tracking based on reference in output load mode from 10 ohms to 5 ohms and (b) based on reference in input voltage mode from 17 to 20 volts

Table 3. Comparative evaluation of control methods for SEPIC converters

Control method	Nonlinear handling	Robustness to disturbance	Response speed	Steady-state accuracy	Overshoot control	Adaptivity	Implementation complexity
Conventional PID [9]	Low	Low–moderate	Moderate	Moderate	Moderate	None	Low
SMC [6]	High	High	Fast	High	Good	Partial	High
Fuzzy logic control (FLC) [15]	High	Moderate	Fast	High	Limited	Partial	Moderate
Model predictive control (MPC) [19]	High	High	Fast	High	Good	High	Very high
Adaptive neural control [20]	Very high	High	Moderate–fast	High	High	Very high	Very high
Proposed IMC–GWO + variable f	High	Very high	Very fast	Very high	Excellent	High	Moderate

FLC and MPC offer better adaptability to nonlinearities. However, MPC requires accurate models and high computational resources, while FLC lacks formal stability assurances. Adaptive neural controllers are flexible and capable of learning but are complex and difficult to train. The proposed IMC-GWO controller with variable switching frequency offers a balanced solution effectively managing nonlinearities, ensuring fast disturbance response, and maintaining overshoot-free voltage tracking. GWO optimization aids in optimal pole placement, while variable frequency improves precision during transients and reduces switching in steady-state. Its efficiency and simplicity make it suitable for real-time embedded power electronic systems. The effect of the PID controller on the SEPIC converter is shown in Table 4.

Table 4. The effect of PID controller on the SEPIC converter

Controller type	Settling time	Overshoot	Rise time	Steady-state error
Proportional control	Small change	Increase	Decrease	Decrease
Integral control	Increase	Increase	Decrease	Delete
Derivative control	Decrease	Decrease	Small change	Ineffective

4. CONCLUSION

This study employed a hybrid control strategy combining a GWO tuned IMC with a variable switching frequency mechanism to achieve reliable and efficient output voltage regulation for the SEPIC converter. The proposed method addresses the challenges associated with SEPIC topology, including non-minimum phase behavior, right-half-plane zero, sensitivity to disturbances, and parameter variability.

Metaheuristic optimization was used to fine-tune the IMC framework for optimal pole placement, enhancing transient response and overall system stability. The variable switching frequency adapted in real time to the magnitude of control error, improving nonlinear performance while minimizing signal saturation and switching losses. Simulation results under diverse operating conditions including step-down and boost modes, noise interference, load transients, and input voltage variations demonstrated fast settling time, minimal overshoot, high tracking accuracy, and strong disturbance rejection. The adaptive switching function enhanced control resolution during transients and maintained output stability in steady-state operation. In conclusion, the proposed control methodology provides a robust and adaptive solution for SEPIC converter regulation, enabling accurate and efficient voltage management in complex, real-world environments through the integration of model-based control, intelligent optimization, and frequency adaptability. The following are suggested as future studies: To investigate different algorithms for controlling the internal model of SEPIC converter and make appropriate load and weather estimations for small- and large-scale renewable energy-based power systems-To investigate smart technology techniques for scheduling for SEPIC converter algorithms to enable optimal reserves to ensure flawless operation of the power system when renewable energy sources are widely integrated.

FUNDING INFORMATION

Authors state no funding involved.

AUTHOR CONTRIBUTIONS STATEMENT

This journal uses the Contributor Roles Taxonomy (CRediT) to recognize individual author contributions, reduce authorship disputes, and facilitate collaboration.

Name of Author	C	M	So	Va	Fo	I	R	D	O	E	Vi	Su	P	Fu
Reza Fazeli	✓	✓	✓	✓	✓		✓		✓			✓	✓	✓
Mohammad Haddad	✓			✓		✓		✓	✓	✓	✓	✓	✓	✓
Zarif Mahmoud Zadehbagheri	✓	✓	✓	✓		✓	✓	✓	✓		✓	✓		✓
Tole Sutikno	✓	✓	✓	✓	✓	✓	✓	✓		✓		✓	✓	

C : **C**onceptualization
M : **M**ethodology
So : **So**ftware
Va : **Va**lidation
Fo : **Fo**rmal analysis
I : **I**nvestigation
R : **R**esources
D : **D**ata Curation
O : Writing - **O**riginal Draft
E : Writing - Review & **E**diting
Vi : **Vi**sualization
Su : **Su**pervision
P : **P**roject administration
Fu : **Fu**nding acquisition

CONFLICT OF INTEREST STATEMENT

Authors state no conflict of interest.

DATA AVAILABILITY

The data that support the findings of this study are available from the corresponding author upon areas.

REFERENCES

[1] M. Verma and S. S. Kumar, "Hardware design of SEPIC converter and its analysis," in *2018 International Conference on Current Trends towards Converging Technologies (ICCTCT)*, Mar. 2018, pp. 1–4, doi: 10.1109/ICCTCT.2018.8551052.

[2] A. Sel, U. Güneş, and C. Kasnakoğlu, "Design of output feedback sliding mode controller for SEPIC converter for robustness," *International Journal of Electronics*, vol. 107, no. 2, pp. 239–249, Feb. 2020, doi: 10.1080/00207217.2019.1643040.

[3] E. Ozsoy, S. Padmanaban, F. Blaabjerg, D. M. Ionel, U. K. Kalla, and M. S. Bhaskar, "Control of high gain modified SEPIC converter: a constant switching frequency modulation sliding mode controlling technique," in *2018 IEEE International Power Electronics and Application Conference and Exposition (PEAC)*, Nov. 2018, pp. 1–6, doi: 10.1109/PEAC.2018.8590246.

[4] B. Chandan, P. Dwivedi, and S. Bose, "Closed loop control of SEPIC DC-DC converter using loop shaping control technique," in *2019 IEEE 10th Control and System Graduate Research Colloquium (ICSGRC)*, Aug. 2019, pp. 20–25, doi: 10.1109/ICSGRC.2019.8837093.

[5] J. E. Salazar-Duque, E. I. Ortiz-Rivera, and J. Gonzalez-Llorente, "Analysis and non-linear control of SEPIC dc-dc converter in photovoltaic systems," in *2015 IEEE Workshop on Power Electronics and Power Quality Applications (PEPQA)*, Jun. 2015, pp. 1–6, doi: 10.1109/PEPQA.2015.7168243.

[6] S. I. Khather and M. A. Ibrahim, "Modeling and simulation of SEPIC controlled converter using PID controller," *International Journal of Power Electronics and Drive Systems (IJPEDS)*, vol. 11, no. 2, pp. 833–843, Jun. 2020, doi: 10.11591/ijpeds.v11.i2.pp833-843.

[7] Y. M. Alsmadi, V. Utkin, M. A. Haj-ahmed, and L. Xu, "Sliding mode control of power converters: DC/DC converters," *International Journal of Control*, vol. 91, no. 11, pp. 2472–2493, Nov. 2018, doi: 10.1080/00207179.2017.1306112.

[8] A. Chabukswar and R. Wandhare, "Adaptive feed-forward reduced-order double-integral sliding mode control of a synchronous SEPIC converter," in *2023 11th National Power Electronics Conference (NPEC)*, Dec. 2023, pp. 1–6, doi: 10.1109/NPEC57805.2023.10384956.

[9] P. K. Gayen, P. R. Chowdhury, and P. K. Dhara, "An improved dynamic performance of bidirectional SEPIC-Zeta converter based battery energy storage system using adaptive sliding mode control technique," *Electric Power Systems Research*, vol. 160, pp. 348–361, Jul. 2018, doi: 10.1016/j.epsr.2018.03.016.

[10] A. M. A. Dalimunthe, I. D. Sara, and Tarmizi, "Adaptive control for SEPIC converter," in *2020 4rd International Conference on Electrical, Telecommunication and Computer Engineering (ELTICOM)*, Sep. 2020, pp. 92–96, doi: 10.1109/ELTICOM50775.2020.9230517.

[11] S. -C. Tan, Y. M. Lai, C. K. Tse, and M. K. H. Cheung, "Adaptive feedforward and feedback control schemes for sliding mode controlled power converters," *IEEE Transactions on Power Electronics*, vol. 21, no. 1, pp. 182–192, Jan. 2006, doi: 10.1109/TPEL.2005.861191.

[12] J.-M. Kwon, W.-Y. Choi, J.-J. Lee, E.-H. Kim, and B.-H. Kwon, "Continuous-conduction-mode SEPIC converter with low reverse-recovery loss for power factor correction," *IEE Proceedings - Electric Power Applications*, vol. 153, no. 5, pp. 673–681, Sep. 2006, doi: 10.1049/ip-epa:20060486.

[13] M. Veerachary, "Control of TI-SEPIC converter for optimal utilization of PV power," in *India International Conference on Power Electronics 2010 (IICPE2010)*, Jan. 2011, pp. 1–5, doi: 10.1109/IICPE.2011.5728087.

[14] R. Moradpour, H. Ardi, and A. Tavakoli, "Design and implementation of a new SEPIC-based high step-up DC/DC converter for renewable energy applications," *IEEE Transactions on Industrial Electronics*, vol. 65, no. 2, pp. 1290–1297, 2017, doi: 10.1109/TIE.2017.2733421.

[15] A. Shawky, T. Takeshita, M. A. Sayed, M. Aly, and E. M. Ahmed, "Improved controller and design method for grid-connected three-phase differential SEPIC inverter," *IEEE Access*, vol. 9, pp. 58689–58705, 2021, doi: 10.1109/ACCESS.2021.3072489.

[16] M. Zadehbagheri, R. Ildarabadi, and M. B. Nejad, "Review of the UPFC different models in recent years," *International Journal of Power Electronics and Drive Systems (IJPEDS)*, vol. 4, no. 3, pp. 343–355, Sep. 2014, doi: 10.11591/ijpeds.v4i3.5982.

[17] M. Al Sakka, J. Van Mierlo, and H. Gualous, "DC/DC converters for electric vehicles," in *Electric Vehicles - Modelling and Simulations*, InTech, 2011, doi: 10.5772/17048.

[18] D. H. Tuan, D. T. Tran, V. N. N. Thanh, and V. V. Huynh, "Load frequency control based on gray wolf optimizer algorithm for modern power systems," *Energies*, vol. 18, no. 4, p. 815, Feb. 2025, doi: 10.3390/en18040815.

[19] B. Gao, H. Guan, W. Shen, and Y. Ye, "Application of the gray wolf optimization algorithm in active disturbance rejection control parameter tuning of an electro-hydraulic servo unit," *Machines*, vol. 10, no. 8, p. 599, Jul. 2022, doi: 10.3390/machines10080599.

[20] M. Zadehbagheri, T. Sutikno, M. J. Kiani, and M. Yousefi, "Designing a power system stabilizer using a hybrid algorithm by genetics and bacteria for the multi-machine power system," *Bulletin of Electrical Engineering and Informatics*, vol. 12, no. 3, pp. 1318–1331, Jun. 2023, doi: 10.11591/eei.v12i3.4704.

[21] M. Dehghan, M. Zadehbagheri, M. J. Kiani, and S. Nejatian, "Virtual power plants planning in the distribution network constrained to system resiliency under extreme weather events," *Energy Reports*, vol. 9, pp. 4243–4256, Dec. 2023, doi: 10.1016/j.egyr.2023.03.080.

[22] M. Zadehbagheri, T. Sutikno, and M. J. Kiani, "A new method of virtual direct torque control of doubly fed induction generator for grid connection," *International Journal of Electrical and Computer Engineering (IJECE)*, vol. 13, no. 1, pp. 1201–1214, Feb. 2023, doi: 10.11591/ijece.v13i1.pp1201-1214.

[23] S. Ghamari, D. Habibi, M. Ghahramani, and A. Aziz, "Design of a robust adaptive cascade fractional-order nonlinear-based controller enhanced using grey wolf optimization for high-power DC/DC dual active bridge converter in electric vehicles," *IET Power Electronics*, vol. 18, no. 1, Jan. 2025, doi: 10.1049/pel2.70056.

[24] G. M. Meseret, R. Kumhar, T. K. Mahato, P. Lakra, B. Kumari, and N. Kumar, "Design of novel secondary controller for AGC in multi-area multi-sources power system incorporated renewable energy using a gray wolf optimizer algorithm," *Engineering Reports*, vol. 7, no. 3, Mar. 2025, doi: 10.1002/eng2.70054.

[25] N. Sridhar and K. S. Kumar, "Integrated control of hybrid PV-wind energy systems using crayfish-optimized neuro-fuzzy inference and a trans Z-source QSEPIC converter," *Iranian Journal of Science and Technology, Transactions of Electrical Engineering*, Aug. 2025, doi: 10.1007/s40998-025-00873-8.

[26] G. Jegadeeswari, D. Lakshmi, and B. Kirubadurai, "Performance enrichment of switched reluctance motors through bio-inspired algorithm for electric propulsion system," *International Review of Applied Sciences and Engineering*, Aug. 2025, doi: 10.1556/1848.2025.01071.

BIOGRAPHIES OF AUTHORS

Reza Fazeli was born in Esfarayen, Iran, in September 1983. In 2008, he received his B.S. in Control Engineering from Islamic Azad University, Mehriz Branch, and an M.S. degree in Control Engineering from Shahrood University of Technology in 2018. He is currently a Ph.D. candidate in Control Engineering at Shahrood University of Technology. His research interests include optimization of control systems, optimization of hybrid systems and classical control, and adaptive control of solar systems. He can be contacted at email: r.fazeli1000@gmail.com.

Mohammad Haddad Zarif earned his Master's degree from City, University of London, where he completed his thesis titled "The Decentralized Determinantal Problem: Necessary Conditions for Its Solvability." His innovative approach to decentralized systems laid the foundation for his advanced research endeavors. He is an Associate Professor of Control Engineering at Shahrood University of Technology, Shahrood, I.R. Iran. His research interests include optimal control, robotic control, and applied computational geometry. He can be contacted at email: mhzarif@shahroodut.ac.ir

Mahmoud Zadehbagheri (Member, IEEE) was born in Yasouj, Iran, in October 1979. He received the B.S. degree in Electrical Engineering from Kashan University in 2003, the M.S. degree in Electrical Engineering from Islamic Azad University, Najafabad Branch, in 2008, and the joint Ph.D. degree in Electrical Engineering from Universiti Teknologi Malaysia (UTM), Johor, Skudai, Malaysia, and Hakim Sabzvari University, Khorasan, Iran, in 2017. He is currently an Associate Professor with the Department of Electrical Engineering, Islamic Azad University, Yasouj Branch. He is a member of the IEEE Smart Grid Community and the IEEE PES Technical Committee. Since 2018, he has served as a co-supervisor and consulting professor for more than 13 Ph.D. and 50 M.Sc. students. He has authored two books, one book chapter, 65 ISI-indexed journal articles, and over 90 conference papers. He is currently collaborating as a reviewer and editorial board member with journals including Applied Energy, International Journal of Hydrogen Energy, IJRER, Micromachines, Sensors, Energy, EPCS, and IJPEDS. His research interests include power electronics, FACTS devices, optimization methods, renewable energy, energy hubs, and power quality. He can be contacted at email: ma.zadehbagheri@iau.ac.ir.

Tole Sutikno is a lecturer and the Head of the Master Program of Electrical Engineering at the Faculty of Industrial Technology at Universitas Ahmad Dahlan (UAD) in Yogyakarta, Indonesia. He received his Bachelor of Engineering from Universitas Diponegoro in 1999, Master of Engineering from Universitas Gadjah Mada in 2004, and Doctor of Philosophy in Electrical Engineering from Universiti Teknologi Malaysia in 2016. All three degrees are in electrical engineering. He has been a Professor at UAD in Yogyakarta, Indonesia, since July 2023, following his tenure as an associate professor in June 2008. He is the current Editor-in-Chief of TELKOMNIKA and Head of the Embedded Systems and Power Electronics Research Group (ESPERG). He is one of the top 2% of researchers worldwide, according to Stanford University and Elsevier BV's list of the most influential scientists from 2021 to the present. His research interests cover digital design, industrial applications, industrial electronics, industrial informatics, power electronics, motor drives, renewable energy, FPGA applications, embedded systems, artificial intelligence, intelligent control, digital libraries, and information technology. He can be contacted at email: tole@te.uad.ac.id.